



Title	Ovarian cysts in MRL/MpJ mice are derived from the extraovarian rete : a developmental study
Author(s)	Lee, Shin-Hyo; Ichii, Osamu; Otsuka, Saori; Elewa, Yaser Hosney; Namiki, Yuka; Hashimoto, Yoshiharu; Kon, Yasuhiro
Citation	Journal of Anatomy, 219(6), 743-755 https://doi.org/10.1111/j.1469-7580.2011.01431.x
Issue Date	2011-12
Doc URL	http://hdl.handle.net/2115/50774
Rights	The definitive version is available at wileyonlinelibrary.com
Type	article (author version)
File Information	JoA219-6_743-755.pdf



[Instructions for use](#)

Title page

Title: Ovarian cysts in MRL/MpJ mice are derived from the extraovarian rete: a developmental study

Authors: Shin-Hyo LEE¹, Osamu ICHII¹, Saori OTSUKA¹, Elewa YH¹, Yuka NAMIKI², Yoshiharu HASHIMOTO², and Yasuhiro KON¹

Affiliations: ¹Laboratory of Anatomy, Department of Biomedical Sciences, Graduate School of Veterinary Medicine, Hokkaido University, Kita 18-Nishi 9, Kita-ku, Sapporo 060-0818, Japan

²Office for Faculty Development and Teaching Enriched Veterinary Medicine, Graduate School of Veterinary Medicine, Hokkaido University, Kita 18-Nishi 9, Kita-ku, Sapporo 060-0818, Japan

Corresponding author: Yasuhiro Kon, DVM, PhD

Laboratory of Anatomy, Department of Biomedical Sciences, Graduate School of Veterinary Medicine, Hokkaido University, Kita 18-Nishi 9, Kita-ku, Sapporo 060-0818, Japan

Tel and Fax: 011-706-5189; E-mail: y-kon@vetmed.hokudai.ac.jp

Running page heading: Sequential morphology of MRL/MpJ mice ovarian cysts

Abstract

MRL/MpJ (MRL) mice, commonly used as a model for autoimmune disease, have a high frequency of ovarian cysts originating from the rete ovarii. In the present study, to clarify how the rete ovarii, which are remnants of mesonephric tubules during embryogenesis, progress to cystic formation with aging, the morphology of MRL rete ovarii was analyzed and compared to that of normal C57BL/6N (B6) mice. In B6 mice, the rete ovarii consisted of a series of tubules including the extraovarian rete (ER), the connecting rete (CR), and the intraovarian rete (IR) based on their location. Although the ER of B6 mice was composed of highly convoluted tubules lined by both ciliated and non-ciliated epithelium, the tubules in the CR and IR had only non-ciliated cells. In MRL mice, dilations of the rete ovarii initiated from the IR rather than the ER or CR. Although the histological types of cells lining the lumen of the rete ovarii were the same as those in B6 mice, the ER in MRL mice showed variety in morphology. In particular, the connections between the ER and ovary tended to disappear with increasing age and the development of ovarian cysts. Furthermore, the epithelium lining large ovarian cysts in MRL mice had ciliated cells forming the cluster. From these findings, it was suggested that cystic changes of the rete ovarii in MRL mice were caused by the dilations of the IR with invasion of the ER and CR into the ovarian medulla. These data provide new pathological mechanisms for ovarian cyst formation.

Keywords: ovarian cysts; rete ovarii; mesonephric tubules; MRL/MpJ mice.

Introduction

The rete ovarii is homologous with the male rete testis and is found in normal adult ovaries of various species including humans. The rete ovarii is formed by mesodermal cells participating in differentiation of the mesonephros that migrate to the developing gonad during embryogenesis (Byskov and Lintern-Moore, 1973). In the adult female, the rete ovarii is described as a tubular structure that connects with the ovary and is present throughout all of life (Wenzel and Odend'hal, 1985). In adult mice, tubules of the rete ovarii are usually localized in the hilus of the ovary, but there have been some cases where it extends through the medulla or is isolated in the parovarian tissues (adipose tissue and connective tissue around the ovary) adjacent to the hilus (Byskov and Lintern-Moor, 1973). In detail, the rete ovarii is divided into three parts in adult mice based on location and morphology: (1) the extraovarian rete (ER), surrounded by the parovarian tissues, is composed of convoluted tubules, (2) the connecting rete (CR) is associated with the smooth muscles of the ovarian ligament, forming a network of convoluted tubules that connects the ER and ovary, and (3) the intraovarian rete (IR) within the ovary (Long, 2002).

In mice, although the presumed function of the rete ovarii is to control the meiosis of germ cells and differentiation of granulosa cells in both the fetus and post-natal female, their function in adults is still unknown (Byskov et al. 1977; Maitland and Ullmann, 1993). On the other hand, a secretory function of the rete ovarii in adults has been suggested by some authors, since secretory materials were observed in the lumen of the rete ovarii, which showed cystic changes in various species such as the

cow, camel, cat, dog, and guinea pig (Byskov, 1975; Jiang et al. 2004). Furthermore, some researchers have hypothesized that the rete ovarii is a common source of ovarian cysts and epithelial tumors in aged mice (Burdette et al. 2007; Fleming et al. 2007; Tan et al. 2005; Tan and Fleming, 2004).

Cysts originating from the rete ovarii in humans are relatively rare compared to follicular cysts; however, ovarian cysts from the rete ovarii could be the source of gynecological problems and result in a medical emergency. In fact, the physical pressure from large cysts on ovarian tissue could induce the interruption of female reproductive functions and hemorrhaging of ruptured cysts (Jain, 2002).

In a previous study, we reported a high incidence of ovarian cysts derived from the rete ovarii in the MRL/MpJ (MRL) mouse strain, a representative model for autoimmune diseases including dermatitis, vasculitis, arthritis, and glomerulonephritis (Ichii et al. 2008; Kon et al. 2008). The ovarian cyst of CD-1 mice, also known as the model of rete ovarian cysts, showed epithelial malformations of cysts such as hyperplasia, metaplasia, stratification, and the appearances of lengthened columnar cells with compact cilia or vacuolated cytoplasm (Fleming et al. 2007; Long, 2002). However, MRL mice in rete ovarian cyst were observed with dilation of the IR mainly composed by single layered squamous or cuboidal epithelium containing ciliated or non-ciliated cells (Kon et al. 2008), and the pathological changes of epithelium were scarce compared to CD-1 mice (Long, 2002). Additionally, a significant genetic linkage was obtained from the analysis of quantitative trait loci (QTL) between specific loci on chromosomes 4 or 14 and the development of ovarian cysts in MRL mice (Lee et al. 2010). On the other hand, there is no evidence as to how the rete ovarii changes

sequentially into an ovarian cyst in this mouse model (Kon et al. 2008; Lee et al. 2010).

In the present study, to clarify the morphological dynamics during ovarian cyst formation in the MRL strain, the three-dimensional features and ultrastructures of the rete ovarii were compared between MRL and normal C57BL/6N (B6) mice at various ages. Our finding indicated a new pathological mechanism: the CR and ER as well as the IR could be a source of ovarian cysts in MRL mice and might contribute to the elucidation of the pathology of female genital problems.

Materials and Methods

Animals

Specific pathogen-free mouse strains of MRL and B6 mice were purchased from Japan SLC (Shizuoka, Hamamatsu). These animals were maintained in a controlled environment with a room temperature of $22 \pm 4^{\circ}\text{C}$, relative humidity of $55 \pm 20\%$, and a 12-h light and dark cycle in the animal facility of the Graduate School of Veterinary Medicine, Hokkaido University. The mice were allowed free access to tap water and an adequate diet. All mice were treated according to the Guidelines for the Care and Use of Laboratory Animals, Hokkaido University, Graduate School of Veterinary Medicine accredited facility by the Association for Assessment and Accreditation of Laboratory Animal Care.

Histology

After inhalation anesthesia of the mice, ovaries with the parovarian tissues in each animal were removed and fixed by a mixture of formalin and acetic acid (70% ethanol : formalin : acetic acid = 15 : 5 : 1). After overnight fixation, specimens were stained with hematoxylin, processed through graded alcohol, and replaced with xylene. The rete ovarii or ovarian cysts were observed and photographed using a stereoscopic microscope, then embedded in paraffin using a routine procedure. Serial sections 4- μm -thick by 30 μm intervals were cut and stained with periodic acid-Schiff's (PAS) and observed under a light microscope. By observing whole serial sections, the CR was identified by both the continuous feature to ER or IR and their epithelial morphology

different from those of adjacent lymphatic ducts, ovarian surface epithelium, and uterine tubes.

Histoplanimetry

To examine the morphological changes of the rete ovarii with age, 35 ovaries from B6 mice and 61 ovaries from 2-weeks-old to 12-months-old MRL mice were analyzed. For histoplanimetry, these mice were divided the examined periods to three groups including 2weeks-3months (before sexual maturation), 4-8 months (after sexual maturation), and 9-12 months (after critical age that all MRL mice develop ovarian cysts (Kon et al. 2008)). The ER phenotype was categorized into 3 types according to the connection with the ovary and complexity of tubular structures. In detail, the absence of tubular structures or undeveloped tubules isolated in the paraovarian tissue was categorized as the regressive type (Fig. 5a). The ER with a single tubule that preserves the connection with the ovary was defined as the simple-tubule type (Fig. 5b). Finally, the ER with well-developed convoluted tubules divided by the lobule was defined as the developed type (Fig. 5c). Using histological sections of the rete ovarii, the ratio of each type of the ER in the total ovary number was calculated in the B6 and MRL mice.

To assess the age-related changes of IR or intraovarian cysts, the maximum sizes of circumference in serial sections were measured by using software Image J (National Institute of Health, Bethesda, MD, USA, <http://www.nig.gov/>), and their averages in each group were calculated. We already confirmed that the maximum circumference of cysts in serial sections as the most appropriate histoplanimetrical indices compared to other indices such as area or diameter in the previous study by QTL analysis (Lee et al.

2010).

Furthermore, each ratio of nuclear/cytoplasm area ratio in ER, CR, and IR epithelium was measured from the histological sections by using software Image J.

Scanning electron microscopy (SEM)

Mice were euthanized by cutting the vena cava under deep anesthesia and perfused thoroughly by heart perfusion with 2.5% glutaraldehyde in 0.1 M phosphate buffer (PB) (pH 7.2). The removed ovaries were then fixed with 2.5% glutaraldehyde in 0.1 M PB for 4 h. Fixed ovaries were cut in a half, rinsed 3 times in 0.1 M PB, and kept in 2% tannic acid for 4 h at 4°C. After washing with 0.1 M PB, these tissues were post-fixed with 1% osmium tetroxide in 0.1 M PB for 4 h. After rinsing with 0.1 M PB, specimens were dehydrated through graded alcohol, transferred into 2-methyl-2-propanol, and freeze-dried. The dried specimens were sputter coated with a Hitachi E-1030 ion sputter coater (Hitachi Co., Ltd., Tokyo, Japan), and then examined on a JEOL S-4100 SEM (Hitachi High-Tech Fielding Corporation, Tokyo, Japan) with an accelerating voltage of 20 kV.

To classify cell types of rete ovarian cysts in MRL mice, the length of primary cilia and cilia on cell surface were measured by using Image J, the mean in each group was calculated (n > 20 cell in each group).

Immunohistochemistry

To examine the proliferation of the rete ovarii epithelium, ovaries with their parovarian tissues were fixed with 4% paraformaldehyde and cut into 2- μ m paraffin

sections. In brief, the endogenous peroxidase of deparaffinized sections was eliminated by incubation of sections in absolute methanol containing 0.3% H_2O_2 for 30 min at room temperature. After blocking solution treatment (Mouse stain kit, Histofine, Nichirei, Tokyo), the sections were incubated overnight at 4°C with the primary antibody for proliferating cell nuclear antigen (PCNA) (Calbiochem, San Diego, CA, USA) diluted in 0.01 M phosphate-buffered saline (PBS). The sections for negative controls were incubated in 0.01 M PBS without primary antibody. Finally, the rete ovarii was visualized with 3, 3'-diaminobenzidine tetrahydrochloride - H_2O_2 solution for 4 min and counterstained with hematoxylin.

Statistics

The non-parametric Kruskal-Wallis test (Schéffe's method) was applied to examine the significance of values among each group.

Results

Structure of the ER in B6 mice

To clarify the normal structure and localization of the rete ovarii in parovarian tissues, the ovaries with adipose tissue in B6 mice were observed using hematoxylin-stained whole-mount specimens and PAS-stained semi-serial sections. As shown in Fig. 1a, most of the rete ovarii was observed outside of the ovary. This unique structure was the ER part of the rete ovarii and prominent from adipose tissue into the peritoneal cavity. In the distal part of the ER, remarkably convoluted tubules were observed (Fig. 1c and d). These tubular structures of the ER showed a clear lumen in whole-mount specimens (Fig. 1d and e). By changing the depth of focus in the stereomicroscope, these tubular structures were determined as closed and coecum (Fig. 1e). The branches of the ovarian vein ran toward the middle of the ER and adipose tissue of the ovary (Fig. 1a). On the other hand, arteries could not be observed due to a lack of blood in the lumen. These morphological findings of the rete ovarii with the parovarian tissues in B6 mice are summarized in Figure 1b.

In paraffin sections, ciliated and non-ciliated epithelial cells (from cuboidal to columnar) lined the convoluted tubules of the ER, and each tubule was separated by a septum of loose connective tissue (Fig. 1g and h). Cellular debris with vacuolated cytoplasm was observed in the lumen, likely from the epithelium (Fig. 1g). Most notably, the mucosal fold, composed of aggregations of stratified or pseudostratified columnar epithelium with cilia, was prominent into the lumen. These tubules of the ER were surrounded by independent serosa that continued to the serosa of the ovary (Fig.

1f-h).

Structure of the CR and IR in B6 mice

As described Long et al. (2002), the ER in the parovarian tissues continues to the CR and IR. Since the CR, without independent serosa, was embedded within the smooth muscle layers of the ovarian ligament, they could only be observed by paraffin sections (Fig. 2a). The epithelium of the CR was composed of stratified or pseudostratified cuboidal epithelium without cilia and a high nuclear/cytoplasm ratio in B6 mice (see Fig 2a, inset).

Relatively, the IR consisted of the shortest part of the rete ovarii. The IR localized in the medullary interstitium, hilus, or serosa of the ovary, and the vessels of medulla were occasionally observed (Fig. 2b). Single-layered non-ciliated cuboidal epithelia of the IR were encircled by the basement membrane distinguishing them from stroma cells (see Fig 2b, inset). Small tubules of the IR showed a clear cytoplasm similar to that of the ER and a lower nuclear/cytoplasm ratio than that of the CR, and these findings were confirmed by histoplanimetry experiments (Fig. 2c).

Structure of the ER in MRL mice

While the ER in B6 mice was composed of several convoluted tubules, the ER of MRL mice showed variations in the number of tubules as well as histological features. Furthermore, the connection between the ER and ovary tended to be lost with aging (Fig. 3a-d). In 2-month-old MRL mice, most of the ER was composed of convoluted tubules continuing to the ovary, and their convolution was simpler than those in B6

mice (Fig. 3a). After sexual maturation, the rete ovarii tended to be dilated (Fig. 3b and c). Slightly dilated ER was connected to the ovarian hilus (Fig. 3b); the connection between the ER and cyst was gone in some mice (Fig. 3c). In older mice that develop large cysts, the parovarian tissues containing vessels were severely pressed by the ovarian cysts, and the ER structures were unclear (Fig. 3d)

Histologically, the ER tubules in MRL mice were lined by flattened or low columnar epithelium with/without cilia. These features differed among individuals and age; however, younger mice tended to have the simple-tubule type that was connected with the ovary, while older mice tended to have the caecal type that was separated from the ovary. The ER having a comparatively wide lumen was occasionally separated from the ovary and lined by cuboidal epithelium with a lot of cell debris or PAS-positive materials in the lumen (Fig. 3e-g). The ER with tubules was composed of cuboidal or low columnar epithelium (Fig. 3g). On the other hand, the ER in MRL mice tended to have an undeveloped mucosal fold structure, compared to that in B6 mice (Fig. 3e-g).

Structures of the CR and IR in MRL mice

The CR in MRL mice was associated with the irregular smooth muscles of ovarian ligaments beside the ovarian hilus and it also dilated with aging (Fig. 4a). The epithelium of the CR was composed of non-ciliated cells, and the expanded lumen of the CR contained cell debris (Fig. 4a).

In young mice (less than 2 months old), the IR started to dilate near the hilus, and their cystic change could not be detected by gross observations (Fig. 4b). Similar to

those of B6 mice, the dilated IR was composed of single-layered flattened epithelium without cilia. In mice with large IR cysts, the connection from the IR to CR and ER could be observed and these showed slight dilations (Fig. 4c).

Although young MRL mice without ovarian cysts tended to show a specific nuclear/cytoplasm ratio among the ER, CR, and IR similar to those in B6 mice, clear identification of the nuclear/cytoplasm ratio in each part of the rete ovarii was impossible due to cell stretching and deformation of the border between the hilus and parovarian tissues in the adult MRL mice.

Correlations between the appearance of the ER and the cyst formation of the IR

Based on the histological observations of MRL rete ovarii, we hypothesized that there is a correlation between the morphological varieties of ER and cyst formation of the IR in MRL mice. For histoplanimetric analysis, the ER was divided into three types by their morphology: 1) the regressive type, where the ER was isolated in parovarian tissues and was composed of undeveloped tubules (Fig. 5a), 2) the simple-tubule type, where the ER was composed of single tubules connecting to the ovary (Fig. 5b), and 3) the developed type, where the ER was composed of multiple convoluted tubules (Fig. 5c).

As shown in Table 1, B6 mice usually had the developed ER type that was composed of complicated convoluted tubules throughout the examined ages. In B6 mice, no relationship between luminal size of the IR and ER type was found, and IR did not dilate with age (Table 1). On the other hand, in MRL mice, there was an increase in the percentage of the regressive ER type with age, indicating that animals with large

cysts tended to show the absence of tubular structures or separation from the ovary. With age, MRL mice showed significant dilation of IR. Furthermore, mice with the regressive ER type had a greater IR circumference (Table 1).

Ultrastructural characteristics of the rete ovarii epithelium and cysts

Under SEM observation, the epithelia of extremely expanded ovarian cysts contained non-ciliated cells and numerous clusters of ciliated cells, which were characteristic of the ER (Fig. 6a and b). The surface of the cyst in aged MRL mice was composed of 3 cell types: Type I cells (non-ciliated), Type II cells (ciliated), and Type III cells. Non-ciliated (Type I) and ciliated cells (Type II) were the same as the cell types observed under a light microscope. Type I cells, which usually possessed primary cilia and sparse microvilli, were divided into dome-like cells and flat-surfaced cells (Fig. 6c and d). Type II cells, with numerous cilia, were usually clustered in a particular space (Fig. 6e), lining the inside of cysts or forming the papillary projections (Fig. 6b). Type III cells, with one or two markedly long curled cilia and relatively longer microvilli, were observed with SEM (Fig. 6f). Morphology of cilia in type III cells was different from that of type II cells, with spiral winding (Fig. 6f). A comparison of cilia length among the three cell types indicated that the cilia of type III cells were remarkably the longest (Fig. 6g).

Detection of cell proliferation in the rete ovarii epithelium of dilated cysts

To examine whether cyst formation was due to the proliferation of epithelium *in situ*, immunohistochemistry for PCNA was performed in 5-month-old and 12-month-

old MRL mice (Fig. 7). Results from these experiments indicated that no proliferating cells were observed in the single-layered cyst epithelium from the rete ovarii of MRL mice within 12 months of age (Fig. 7a-d).

Discussion

Normal mice preserve the structures of the rete ovarii throughout their life.

In embryogenesis, some part of mesonephrogenic cells forms the mesonephric tubules at the cranial pole of the developing ovary, which remains as the rete ovarii in the adult female (Waterberg 1982). Similar to previous reports (Long 2002), by observation of the three-dimensional morphology of the rete ovarii in the B6 strain of mice, we confirmed that the rete ovarii structure in normal adult mice is divided into the ER, CR, and IR by their localization in the ovary and parovarian tissues. Furthermore, ruminants had the connections between rete ovarii and infundibulum of the uterine tubule (Odend'hal et al., 1986), we could not find the connections between rete ovarii and uterine tube in both C57BL/6 and MRL/MpJ mice in this study. The epithelium lining the rete ovarii is composed of non-ciliated cuboidal to columnar cells, non-ciliated pseudostratified or multilayered cuboidal cells, and ciliated and non-ciliated columnar cells in the IR, CR, and ER, respectively. Furthermore, the ER had highly convoluted tubules and prominent mucosal folds, and these structures were not dramatically changed throughout the examined ages of B6 mice. Our findings indicate normal B6 mice, resistant to cystic rete ovarii, tend to preserve the structures of the rete ovarii, rather than have it be regressed. Although the fetal rete ovarii cells influence development of the ovary through interaction with other cellular constituents and differentiate to form follicular cells (Upadhyay et al. 1979; Wenzel and Odend'hal, 1985), the function of the remaining rete ovarii in adult females is unclear. In the present study, we clarified the PAS-positive materials, papillary mucosal fold, and

prominent ciliated columnar cells in the ER lumen of normal B6 mice, similar to previous reports in various species (Archbald et al. 1971; Byskov 1975; Byskov 1978; Gelberg et al. 1984). These findings suggest a secretory function of the rete ovarii; however, further studies using real-time observation, such as video recording of cilia and fluid movement in the organ culture medium, would be needed to further investigate this hypothesis.

The CR and ER structures participate in intraovarian cyst formation in MRL mice

The majority of rete ovarii cysts in MRL mice are located within or adjacent to the hilus of the ovary (Kon et al. 2008; Lee et al. 2010). In addition to these findings, we clarified that the initial cyst formation in MRL mice was identified as IR expansion. Usually, the dilations of IR in MRL mice were started from after sexual maturation (Table 1). Furthermore, MRL mice showed polymorphism in the ER, which could be divided into the regressive, simple, and developed types. In MRL mice, the structure of ER tubules regressed with age, in contrast to those in B6 mice. From these findings, we hypothesized that there was a correlation between ER phenotype and IR dilation. Indeed, data from our correlation analysis between ER phenotype and IR size demonstrated that the ovaries with a less-developed ER structure tended to have larger cysts in MRL mice.

Furthermore, although the IR in MRL mice was lined by non-ciliated cells similar to those in B6 mice, large ovarian cysts occupying over half of the ovarian stroma had patchy clusters of ciliated columnar cells, which were a typical feature of the ER. Similar to these findings, Kon et al. (2008) clarified the ciliated cells in the ovarian cyst

epithelium by both light microscopy and transmission electron microscopies. Based on the localization of ciliated cells in ovarian cysts, we propose possible pathological changes of ovarian cyst formation in MRL mice (Fig. 8). In the early phase, the IR epithelium stretches and forms a small cyst because of an increase in internal pressure by unknown causes such as excessive secretion or defective re-absorption and abnormal fluid movement in entire rete tubules (Fig. 8b). Then, the CR epithelium continuing from the IR becomes part of the intraovarian cyst (Fig. 8b). With involution of the CR, the convoluted tubular structure of the ER inevitably becomes less convoluted and contributes to the cyst formation (Fig. 8b and c). Furthermore, cyst epithelium in ovarian stroma within 1-year-old MRL mice was not proliferative based on PCNA immunohistochemistry data. These data indicate that the formation of cysts was not caused by the proliferation of epithelium in the rete ovarii. However, a minority of MRL mice with multiple rete tubules seemed to form ovarian cysts yielding to internal pressure at the critical point because there are some cases of multiple cysts with apparent septum structures (Fig. 8d and e).

Possible primary causes of ovarian cysts in MRL mice

Although we have proposed a mechanism for ovarian cyst formation, the primary causes remain unclear. Recently, it was noted that embryonic metabolism was retained in adult MRL mice and this unique phenotype is associated with tissue remodeling (Naviaux et al. 2009). By 10.5 embryonic days in mice, tubules emerge from the mesonephric duct, then between 11.5 and 13.5 embryonic days, convoluted mesonephric tubules are bound to the mesonephric duct (Vuzquez et al. 1998). It has

been reported that slight misalignment in embryogenesis might be involved in late mesonephric duct tissue remodeling, dilated epididymal ducts, rete testis dilation, and multicystic kidneys (Smith et al. 2008; Nistal et al. 2010). From these findings, abnormal cellular metabolisms in MRL strain might affect tissue organization from mesenchymal origin and the differentiation of the mesonephric duct in embryogenesis. Therefore, polymorphism of the ER associated with the formation of cysts in MRL mice might be a result of abnormal events in embryogenesis.

In addition to ciliated and non-ciliated cell types lining the cyst lumen in histological sections, we found a third cell type that had one or two curly cilia in cells and a dense and long microvilli population. Although the significant functions and origins were not clear in this study, the developmental role of cilia has been emphasized in cystic diseases of various organs. Hydrocephalus and polycystic kidney disease are interpreted as cilia-associated diseases such as primary ciliary dyskinesia or immotile cilia syndrome, which involve a malfunction of the primary cilia or cilium of epithelia enclosing the ventricles or urinary tubules (Lechtreck et al. 2008; Boehlke et al. 2010; Gallagher et al. 2010). From these findings, we hypothesize that the primary cilia or cilium of the rete ovarii epithelium have a role in homeostasis of the rete ovarii in adults, and dysfunctions of these cilia might cause abnormal fluid mechanics. In addition to the functions of epithelium associated with the regulation of fluid mechanics, chronic inflammation associated with autoimmune traits of adult MRL mice might result in abnormal fluid excretion of the rete ovarii epithelium. In mucosal epithelium such as the gastrointestinal tract, inflammatory cytokines stimulated the secretion of mucus and fluid (Rege, 1999).

In summary, we clarified that MRL ovarian cysts initiated from dilation of the IR, and these pathological events involved the CR and ER as a part of the cysts. This result might provide fundamental information about the pathogenesis of ovarian cysts, which is a major female reproduction problem.

References

- Archbald LF, Schultz RH, Fahning ML, Kurtz HJ and Zemjanis R** (1971) Rete ovarii in heifers: a preliminary study. *J Reprod Fertil* **26**, 413-414
- Boehlke C, Kotsis F, Patel V, et al.** (2010) Primary cilia regulate mTORC1 activity and cell size through Lkb1. *Nat Cell Biol* **12**, 1115-1122
- Burdette JE, Oliver RM, Ulyanov V, et al.** (2007) Ovarian epithelial inclusion cysts in chronically superovulated CD1 and Smad2 dominant-negative mice. *Endocrinology* **148**, 2598-2604
- Byskov AG and Lintern-Moore S.** (1973) Follicle formation in the immature mouse ovary: the role of the rete ovarii. *J Anat* **116**, 207-217
- Byskov AG** (1975) The role of the rete ovarii in meiosis and follicle formation in the cat, mink, and ferret. *J Reprod Fert* **45**, 201-209
- Byskov AG, Skakkebaek NE, Stafanger G, et al.** (1977) Influence of ovarian surface epithelium and rete ovarii on follicle formation. *J Anat* **123**, 77-86
- Byskov AG** (1978) The anatomy and ultrastructure of the rete system in the fetal mouse ovary. *Biol Reprod* **19**, 720-735
- Fleming JS, McQuillan HJ, Millier MJ, et al.** (2007) E-cadherin expression and bromodeoxyuridine incorporation during development of ovarian inclusion cysts in age-matched breeder and incessantly ovulated CD-1 mice. *Reprod Biol Endocrinol* **5**, 1-14
- Gallagher AR, Germino GG, Somlo S** (2010) Molecular advances in autosomal dominant polycystic kidney disease. *Adv Chronic Kidney Dis* **17**, 118-130

Ichii O, Konno A, Sasaki N, et al. (2008) Autoimmune glomerulonephritis induced in congenic mouse strain carrying telomeric region of chromosome 1 derived from MRL/MpJ. *Histol Histopathol* **23**, 411-422

Jain KA (2002) Sonographic spectrum of hemorrhagic ovarian cysts. *J Ultrasound Med* **21**, 879-886

Jiang J, Take Y, Kobayashi Y, et al. (2004) Adenomatous hyperplasia of the rete ovarii in beagle. *J Toxicol Pathol* **17**, 127-128

Kon Y, Konno A, Hashimoto Y, et al. (2008) Ovarian cysts in MRL/MpJ mice originate from rete ovarii. *Anat Histol Embryol* **36**, 172-178

Lehtreck KF, Delmotte P, Robinson ML, et al. (2008) Mutations in Hydin impair ciliary motility in mice. *J Cell Biol* **11**, 633-643

Lee S, Ichii O, Otsuka S, et al. (2010) Quantitative trait locus analysis of ovarian cysts derived from rete ovarii in MRL/MpJ mice. *Mamm Genome* **21**, 162-171

Long GG (2002) Apparent mesonephric duct (rete analge) origin for cysts and proliferative epithelial lesions in the mouse. *Toxicol Pathol* **30**, 592- 598

Maitland P and Ullmann SL. (1993) Gonadal development in the opossum, *Monodelphis domestica*: the rete ovarii does not contribute to the steroidogenic tissues. *J Anat* **183**, 43-56

Naviaux RK, Le TP, Bedelbaeva K, et al. (2009) Retained features of embryonic metabolism in the adult MRL mouse. *Mol Genet Metab* **96**, 133-144

Nistal M, González-Peramato P, Sousa G, et al. (2010) Cystic dysplasia of the epididymis: a disorder of mesonephric differentiation associated with renal maldevelopment. *Virchows Arch* **456**, 695-702

- Odend'hal S, Wenzel JS and Player EC** (1986) The rete ovarii of cattle and deer communicates with the uterine tube. *Anat Rec* **216**, 40-43
- Rege RK** (1999) Inflammatory cytokines alter human gallbladder epithelial cell absorption/secretion. *J Gastrointest Surg* **4**, 185-192
- Smith PJ, DeSouza R, Roth DR** (2008) Cystic dysplasia of the rete testis. *Urology* **72**, 237-240
- Tan OL, Hurst PR, Fleming JS** (2005) Location of inclusion cysts in mouse ovaries in relation to age, pregnancy, and total ovulation number: implications for ovarian cancer? *J Pathol* **205**, 483-490
- Tan OL and Fleming JS.** (2004) Proliferating cell nuclear antigen immuno-reactivity in the ovarian surface epithelium of mice of varying ages and total lifetime ovulation number following ovulation. *Biol Reprod* **71**, 1501-1507
- Upadhyay S, Luciani JM and Zamboni L** (1979) The role of the mesonephros in the development of indifferent gonads and ovaries of the mouse. *Ann Biol Anim Biochem Biophys* **19**, 1179-1196
- Vuquez MD, Bouchet P, Mallet JL, et al.** (1998) 3D reconstruction of the mouse's mesonephros. *Anat Histol Embryol* **27**, 283-287
- Wenzel JG and Odend'hal S.** (1985) The mammalian rete ovarii: a literature review. *Conell Vet* **75**, 411-425
- Waterberg H** (1982) Development of the early human ovary and role of the mesonephros in the differentiation of the cortex. *Ant Embryol* **165**, 253-280

Figure legends

Fig. 1. Structures of the extraovarian part of the rete ovarii in B6 mice. **a.** In whole-mount preparation at 2-month-old, ER structure is observed besides the ovary (Ov). Ovarian vein (arrowheads) and its branches (arrows) are observed in the adipose body (AB) running toward the ER. The hilus where rete system starts is located on the opposite side from the front. Bar = 1 mm. Od: oviduct. **b.** Schematic drawing of comparative localization of the rete ovarii tubules in B6 mice. From the ventral to the dorsal aspect, the ER turns out of the ovary forming an arch, almost all parts are buried deep in the adipose body, except for the limited area of the distal end. **c.** Adipose tissues were removed from the ER in a 2-month-old mouse. Highly convoluted tubules are contained within the ER structure. The rete ovarii branch of the ovarian vein (arrow) is closely associated with the ER. Hematoxylin stain. Bar = 1 mm. **d-e.** In whole-mount preparation removed adipose tissues at 12-month-old, distal ends of the ER (arrows) are ramified into several convoluted tubules and surrounded by thick connective tissues densely stained with hematoxylin. Hematoxylin stain. Bars = 1 mm. **f-h.** Microscopic features of the ER in the same 12-month-old mouse. PAS-hematoxylin stain. Bars = 200 μ m. **f.** The ER (dotted box) is localized at outside of the ovarian bursa. **g.** In magnified figure, ciliated pseudostratified or stratified columnar epithelia form mucosal folds toward the lumen (arrow), in which cell debris (arrowhead) are observed. **h.** Proximal parts of the rete ovarii are more convoluted and lobular in appearance and are surrounded by loose connective tissue (arrowheads).

Fig. 2. Microscopic features of the rete ovarii in B6 mice. **a.** Longitudinal section of the CR in a 12-month-old mouse. The CR is closely associated with the ovarian ligament (arrowheads), and their epithelial border shows an irregular line and the basement membrane is discontinuous. The inset shows high magnification of the epithelium. PAS-hematoxylin stain. Bar = 200 μ m. **b.** Cross (arrow) and longitudinal sections (arrowhead) of the IR in a 5-month-old mouse. Lumen of the IR is narrow and the basement membrane is clear. The inset shows high magnification of the epithelium. PAS-hematoxylin stain. S: stroma cells, V: small vein. Bar = 200 μ m. **c.** Nuclear/cytoplasm ratio in each part of the IR, CR, and ER. *: $P < 0.0001$ by the Kruskal-Wallis test, Schéffe's method, $n > 30$ cells in each group, value = means \pm S.E.

Fig. 3. Structures of the ER and ovarian cysts in MRL mice. **a-d.** Whole-mount preparations stained by hematoxylin. Bars = 1 mm. **a.** At 2-month-old, a singular tubule of the ER (black arrow) connects the distal end of the ER (white arrowhead), surrounded by thick connective tissue. **b.** At 4-month-old, the ER is dilated and continues to the small cyst near the hilus. Yellow dotted line shows ovarian rete system. **c.** At 3-month-old, the rete ovarii branch of the ovarian vein (arrowheads) and disconnected distal end of the ER (arrow) are observed in the parovarian tissues. **d.** At 10-month-old, the parovarian tissues and the ovarian veinous branches (arrows) seem to be attached to the cyst wall due to significant cyst development. C: cysts, Od: oviduct, Ov: ovary, Ut: uterine. **e-g.** Histological sections stained by PAS-hematoxylin. Bars = 200 μ m. **e.** At 3-month-old, the distal end of the ER is surrounded by thick connective tissue and independent serosa and is composed of non-ciliated cuboidal

epithelium (arrow and inset). Arrowhead indicates the CR associated with the ovarian ligament. Some parts of the adipose tissue were removed. **f.** At 5-month-old, PAS-positive material (arrows) is shown in the ER lumen. **g.** The epithelia are highly ciliated (inset). Serosa and adipose tissues were removed. At 7-month-old, cuboidal to low columnar epithelium with or without cilia are observed at a single tubular ER (arrow and inset).

Fig. 4. Microscopic features of the CR and IR in MRL mice. **a-c.** Histological sections stained by PAS-hematoxylin. Bars = 200 μ m. **a.** At 6-month-old, cell debris in the lumen of the dilated CR (asterisk) is detected (panel a). The inset shows high magnification of the epithelium. At 2-month-old, expansion of the IR (single asterisk) and slightly dilated ER (double asterisks) are observed. The inset shows high magnification of flattened epithelium of the IR (panel b). At 4-month-old, amorphous cyst (single asterisk) with dense PAS-positive materials (arrows) expanded toward the ovarian ligament and adipose tissues, and invades into intraovarian cyst (double asterisks) (panel c).

Fig. 5. Histological typing of ER. PAS-hematoxylin stain. **a.** Discontinuous ER is categorized as “regressive type”. **b.** A single convoluted ER is categorized as “simple type”. **c.** Complicated ER is categorized as “developed type”. Bars = 200 μ m.

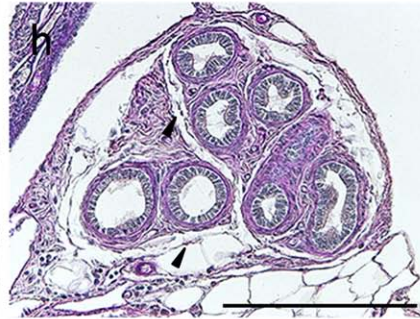
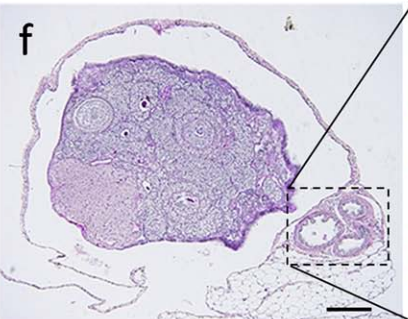
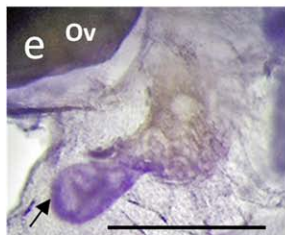
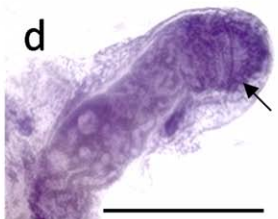
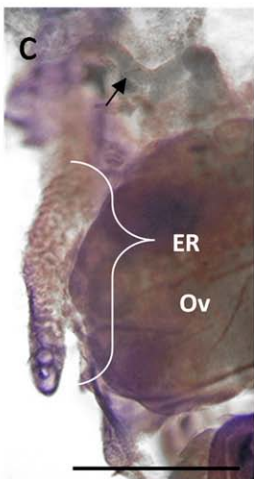
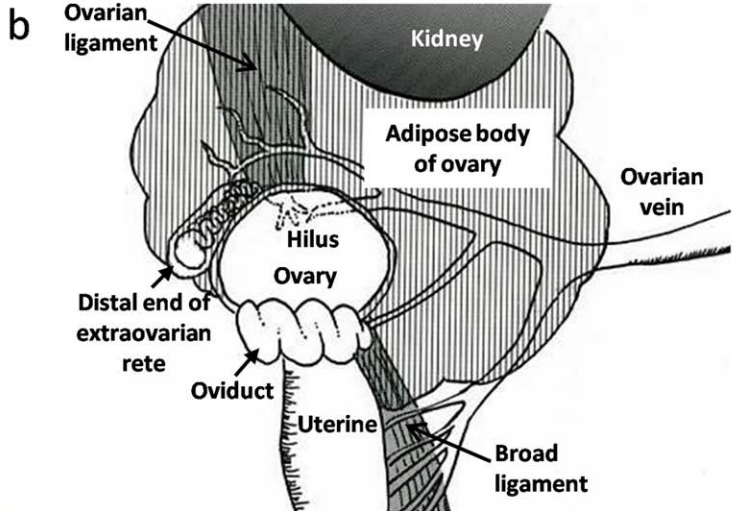
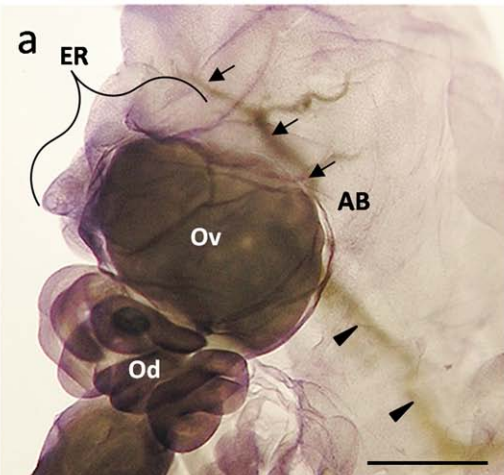
Fig. 6. Scanning electron microscopic observation of ovarian cysts in 12-month-old MRL mice. **a.** Cyst epithelium is composed of ciliated and non-ciliated cells. **b.** Papillary structures (white arrowheads) are observed in the cyst wall, in which ciliated and non-

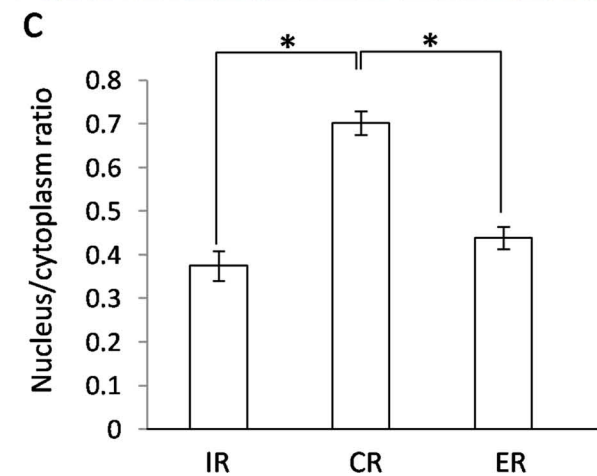
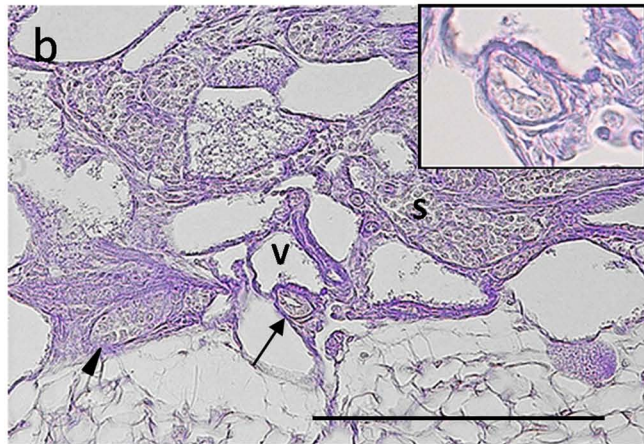
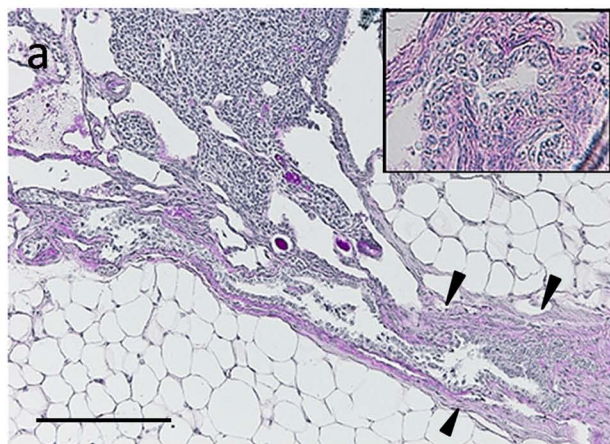
ciliated cells are co-localized. **c-f.** Epithelial cells making up the ovarian cyst wall are classified into 3 groups. Bars = 10 μ m. **c and d.** Type I (non-ciliated) is composed of dome-like cells (c) and flattened cells (d) with primary cilia and low microvilli. **e.** Typical ciliated cells are categorized as type II cells. Long cilia indicated by the white arrowheads are different from type II cells. **f.** One or two curly cilia longer than normal cilia of ciliated cells are discriminated as type III cells, in which dense and tall microvilli are observed in the cell surface (white arrow). **g.** Comparison of cilia length of type I cells, type II cells, and type III cells. *: $P < 0.0001$ by the Kruskal-Wallis test, Schéffe's method, $n > 20$ cells in each group, values = means \pm S.E.

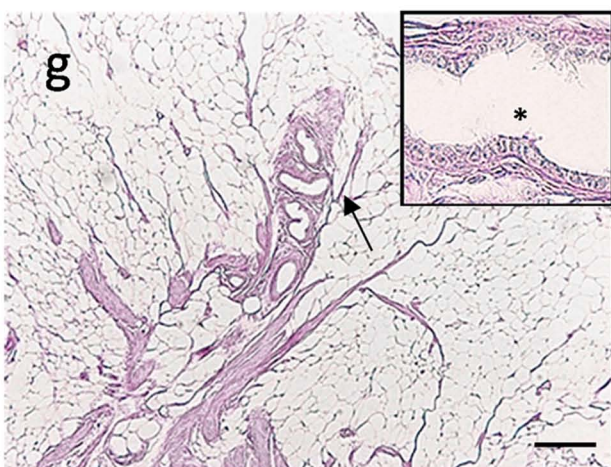
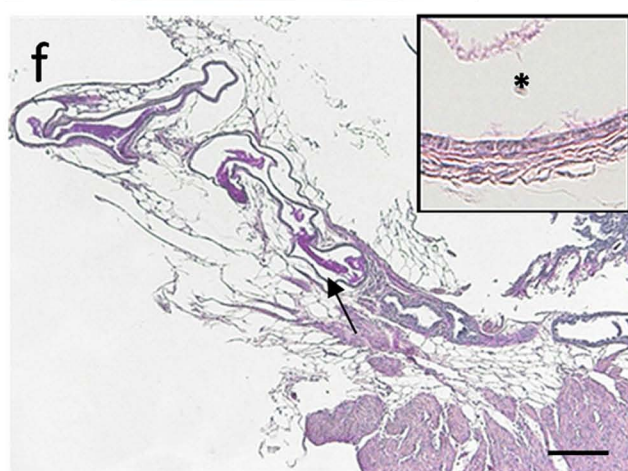
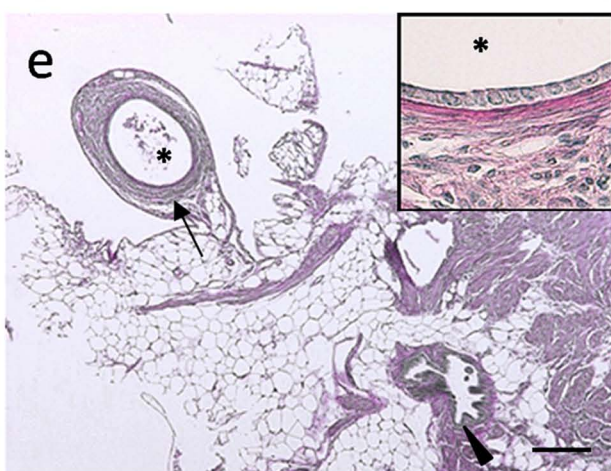
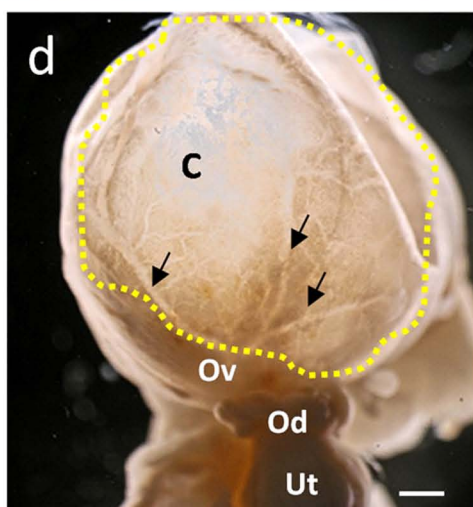
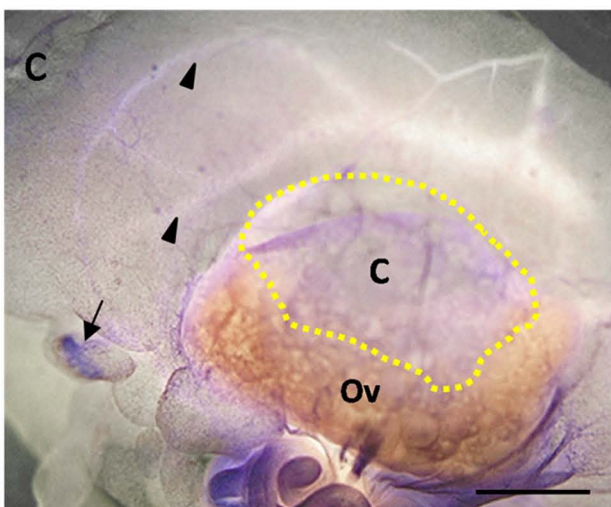
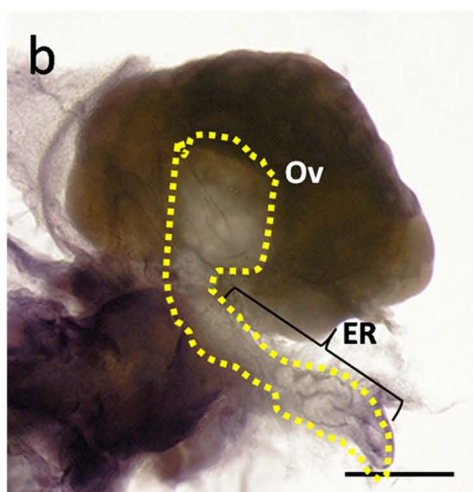
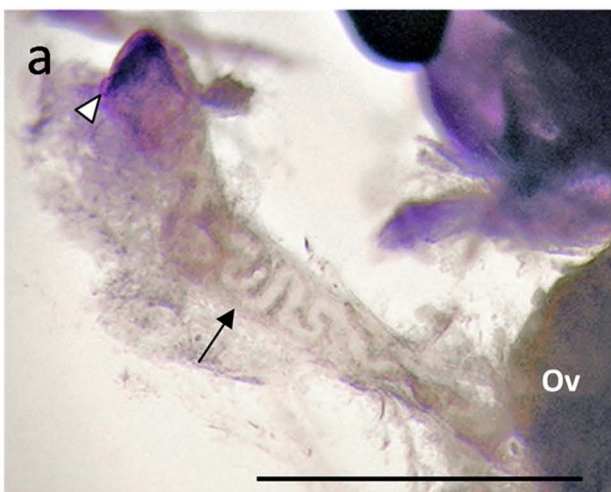
Fig. 7. Detection of PCNA-positive cells in the MRL ovarian cysts. **a-b.** 5-month-old. **c-e.** 12-month-old. PCNA-positive epithelial cells are detected neither at 5-month-old (a and b) nor at 12-month-old (c-e). Arrowheads indicate the epithelium lining the ovarian cysts derived from rete ovarii (a-e), and arrow indicates the follicular epithelial cells showing PCNA positive reaction (h). Bars = 200 μ m.

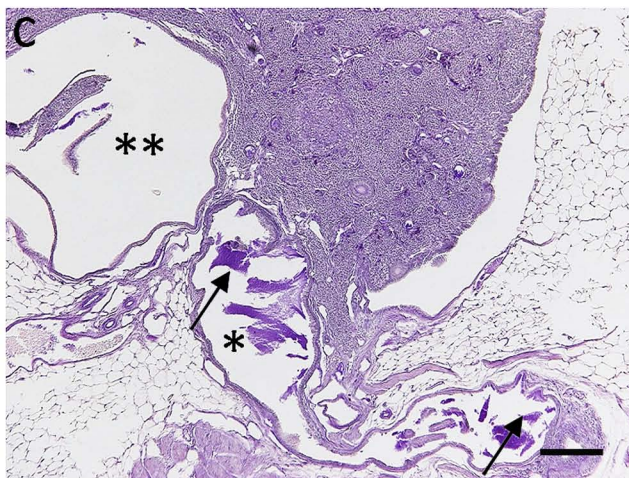
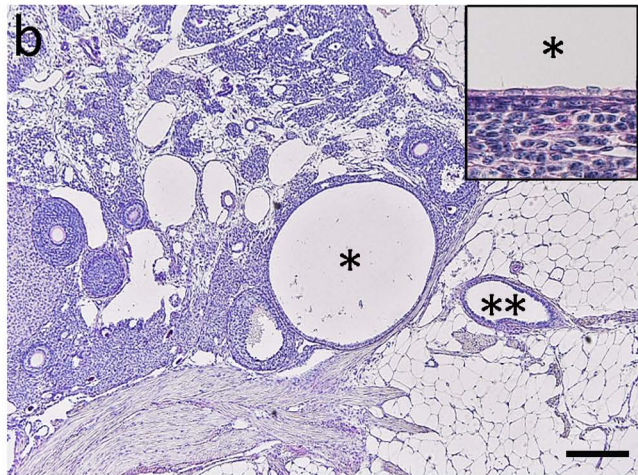
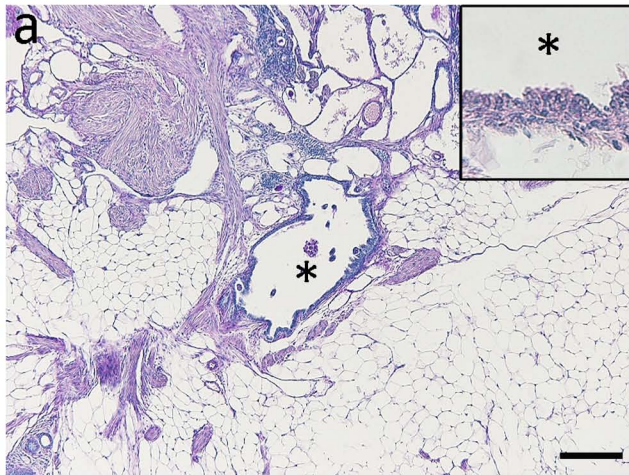
Fig. 8. Schematic drawings of time-interval change of the rete ovarii in MRL mice from the lateral to the medial aspect. The direction of arrows indicates the relative positions of ovary. AB: adipose body of the ovary, C: cyst, CR: the connecting rete, ER: the extraovarian rete, ER': separated ER, H: hilus, IR: the intraovarian rete, OL: ovarian ligament. **a.** Mice less than 2 months old typically do not have a dilated IR. **b-c.** MRL mice from 3 to 12 months of age. **b.** Distal part of the ER becomes tracked towards the ovarian ligament and is disconnected in some mice. **c.** In large cysts, ciliated cells (white

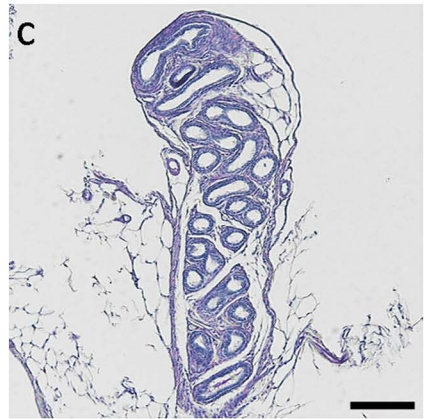
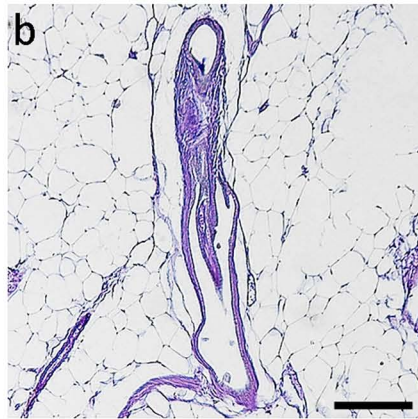
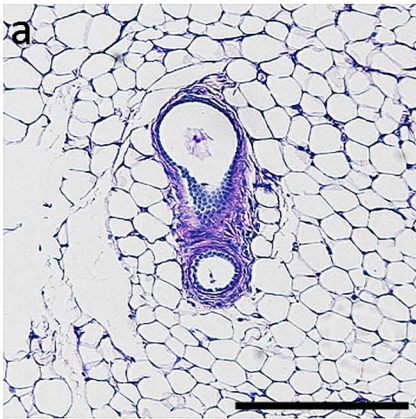
arrows) appear in the rete epithelium around the hilus. **d-e**. Multiple cyst formation in a few MRL mice. **d**. In the early phase, MRL mice with several ER tubules, as in the B6 mice, would be more resistant to ER inclusion than MRL mice with a singular and disconnected ER. **e**. Eventually, several tubules of the ER form multiple ovarian cysts in the ovary and ovarian ligament.

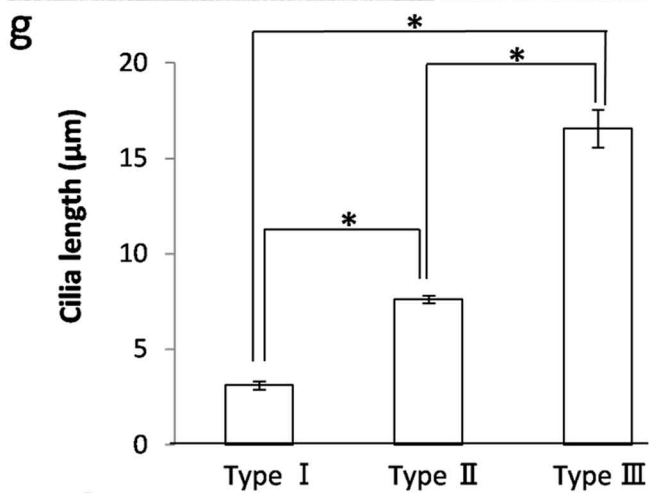
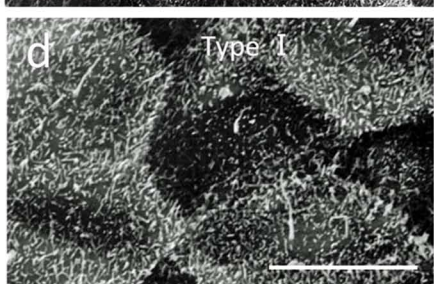
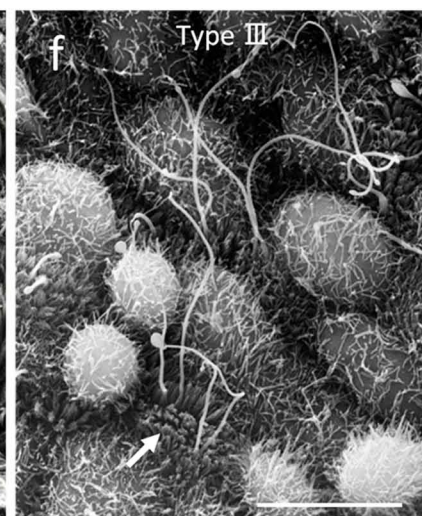
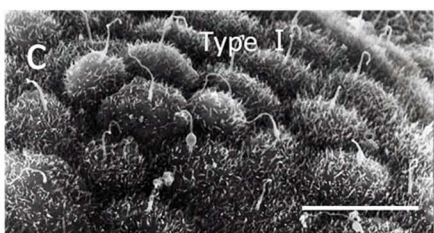
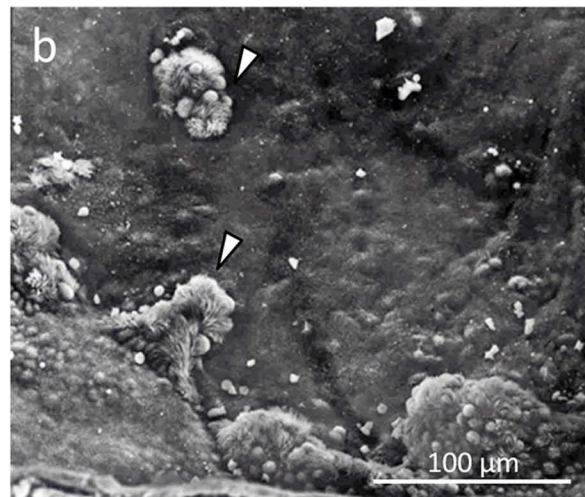


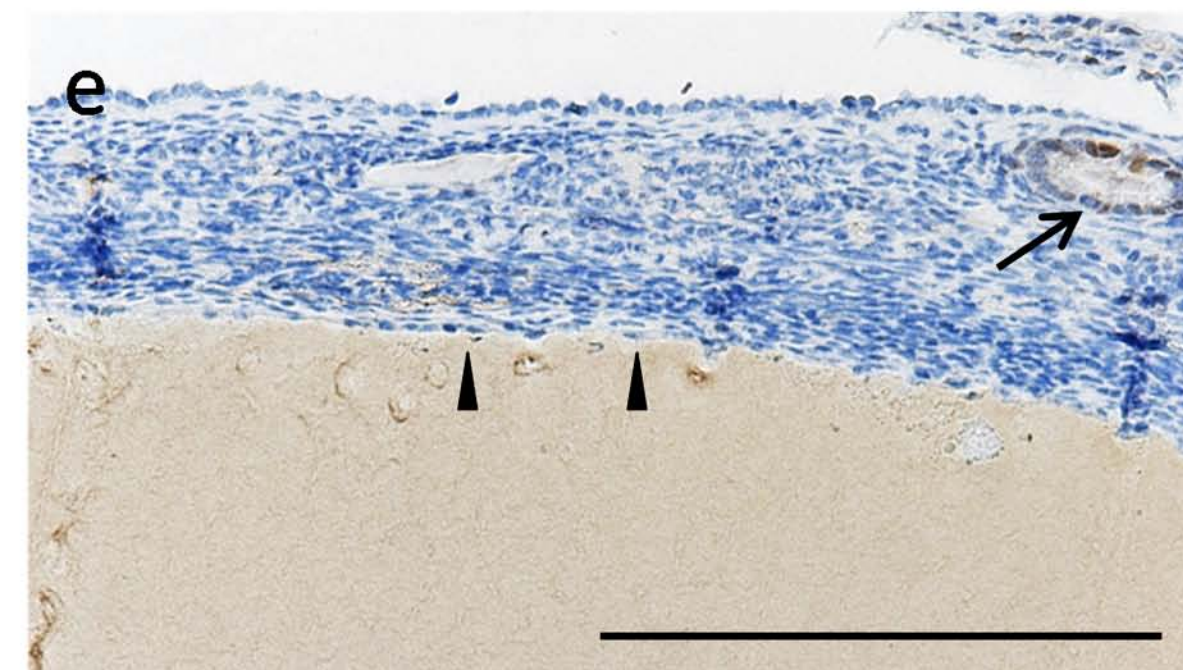
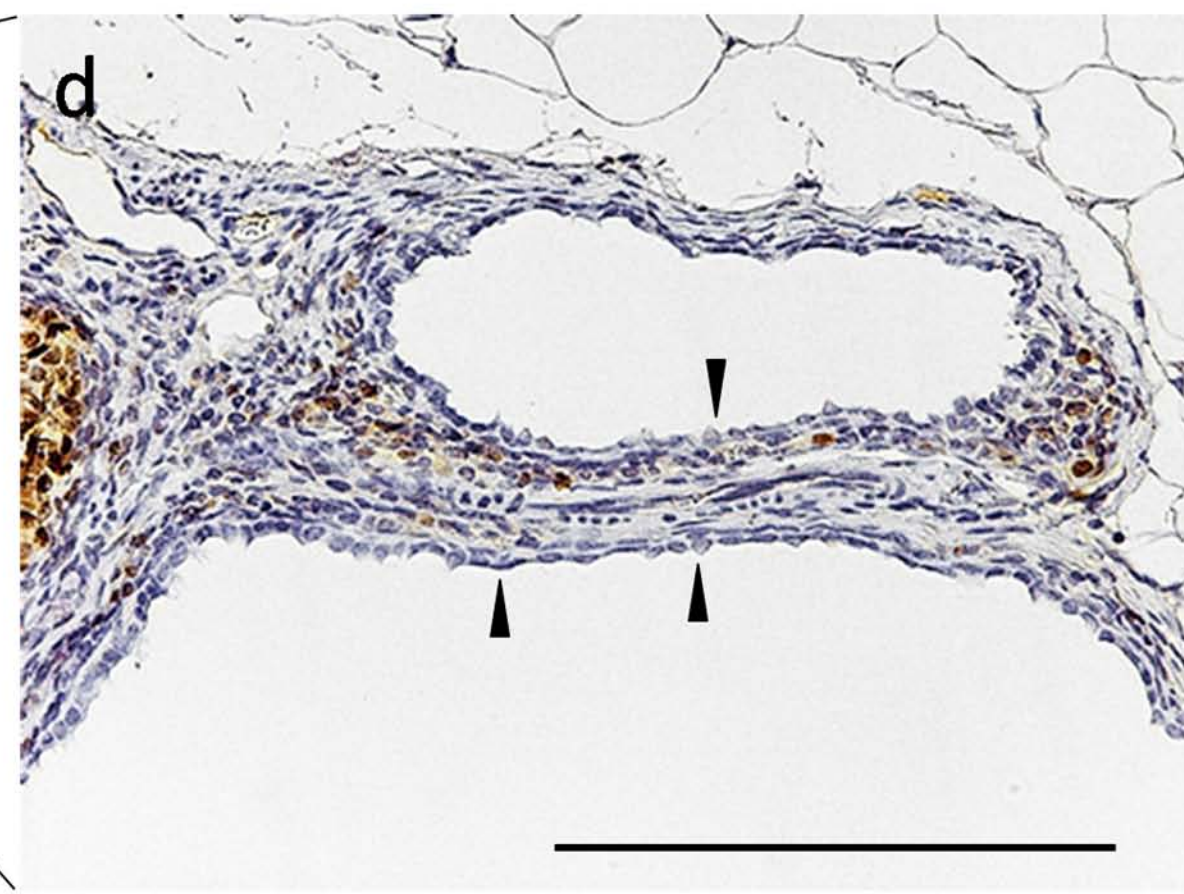
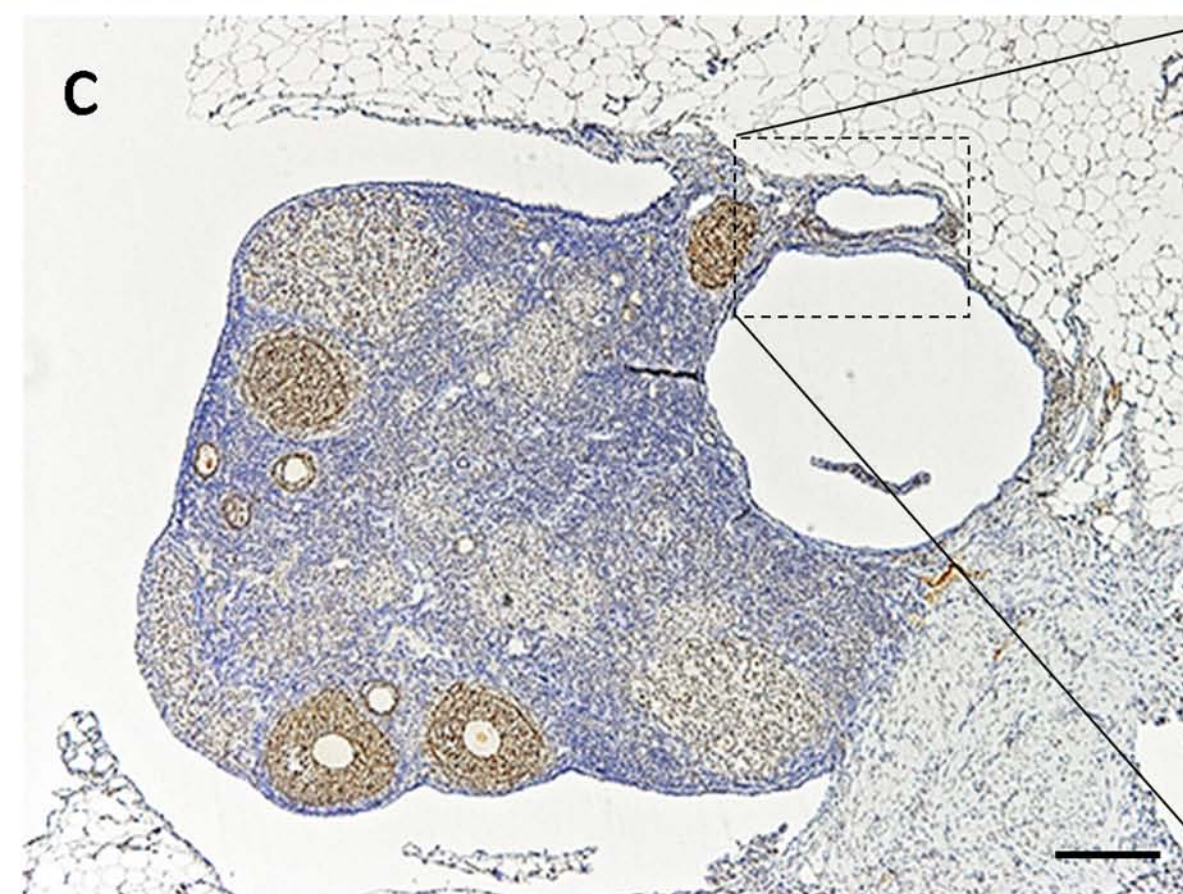
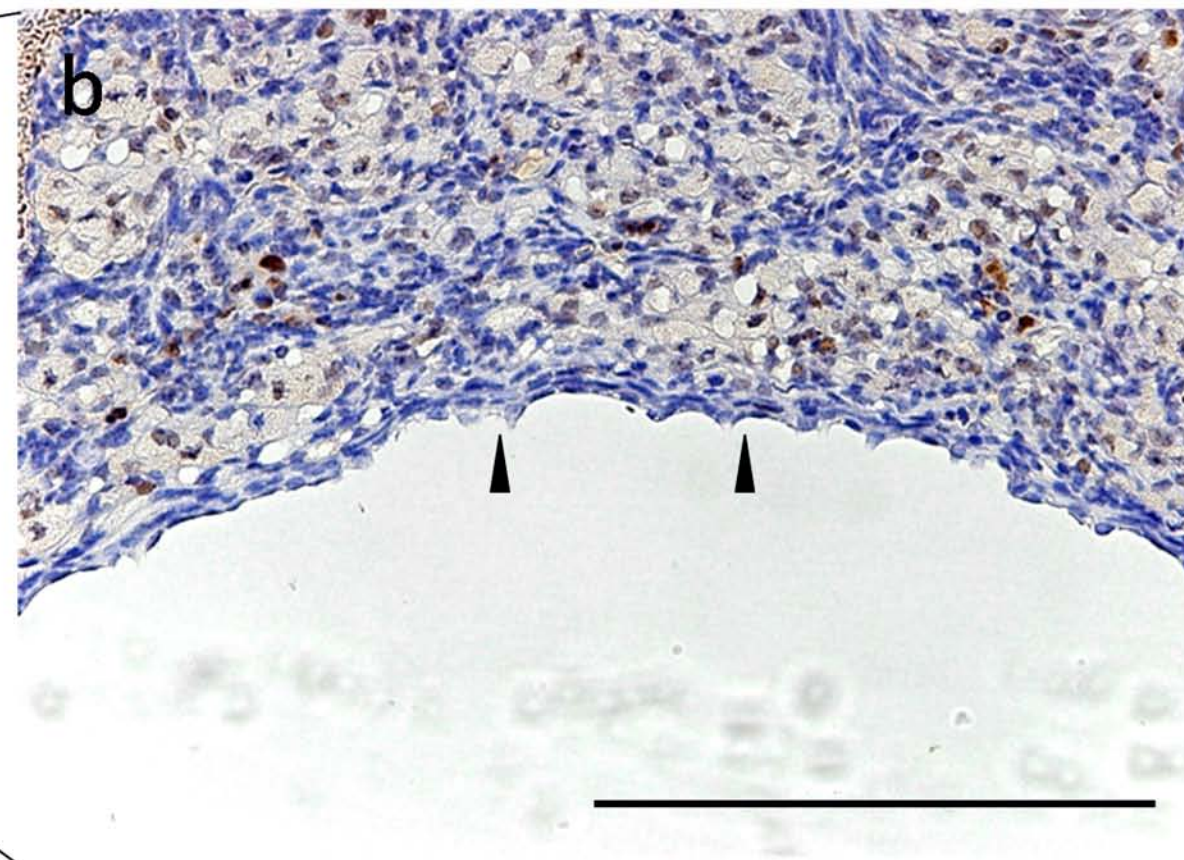
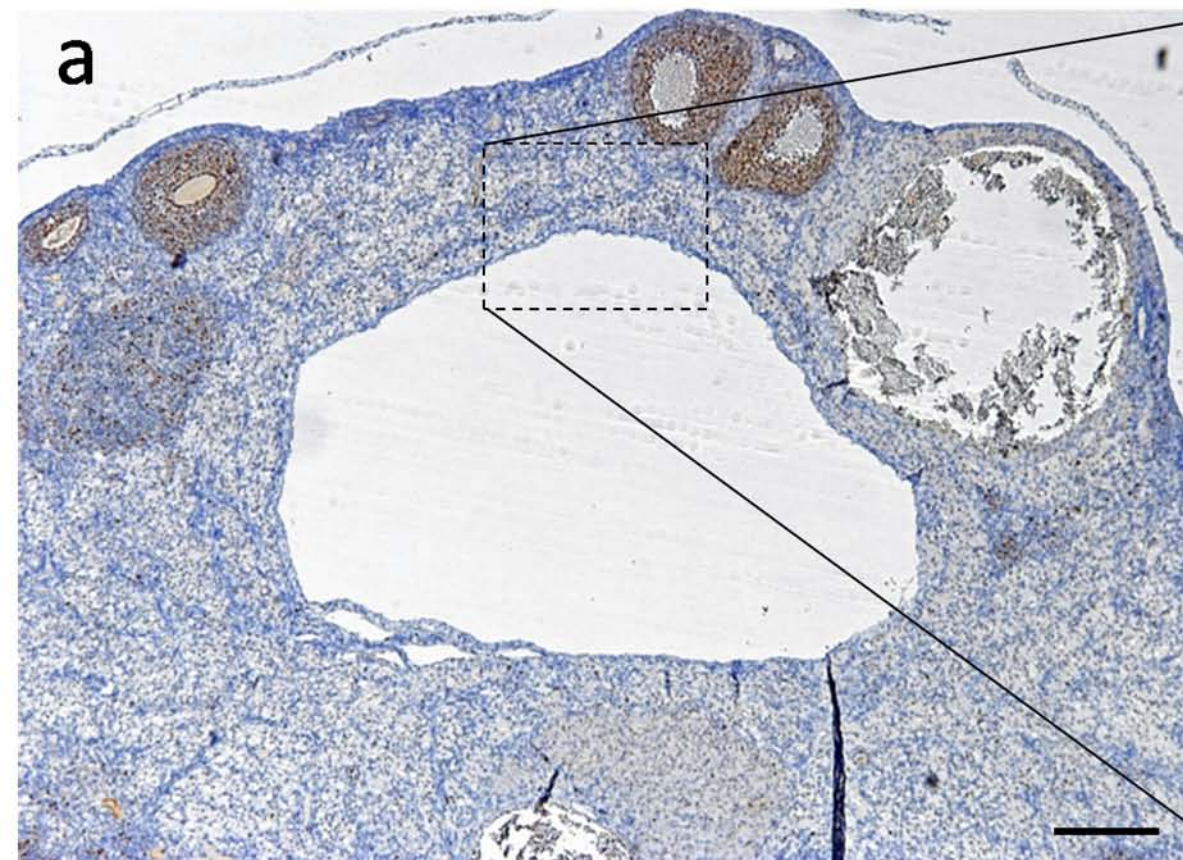












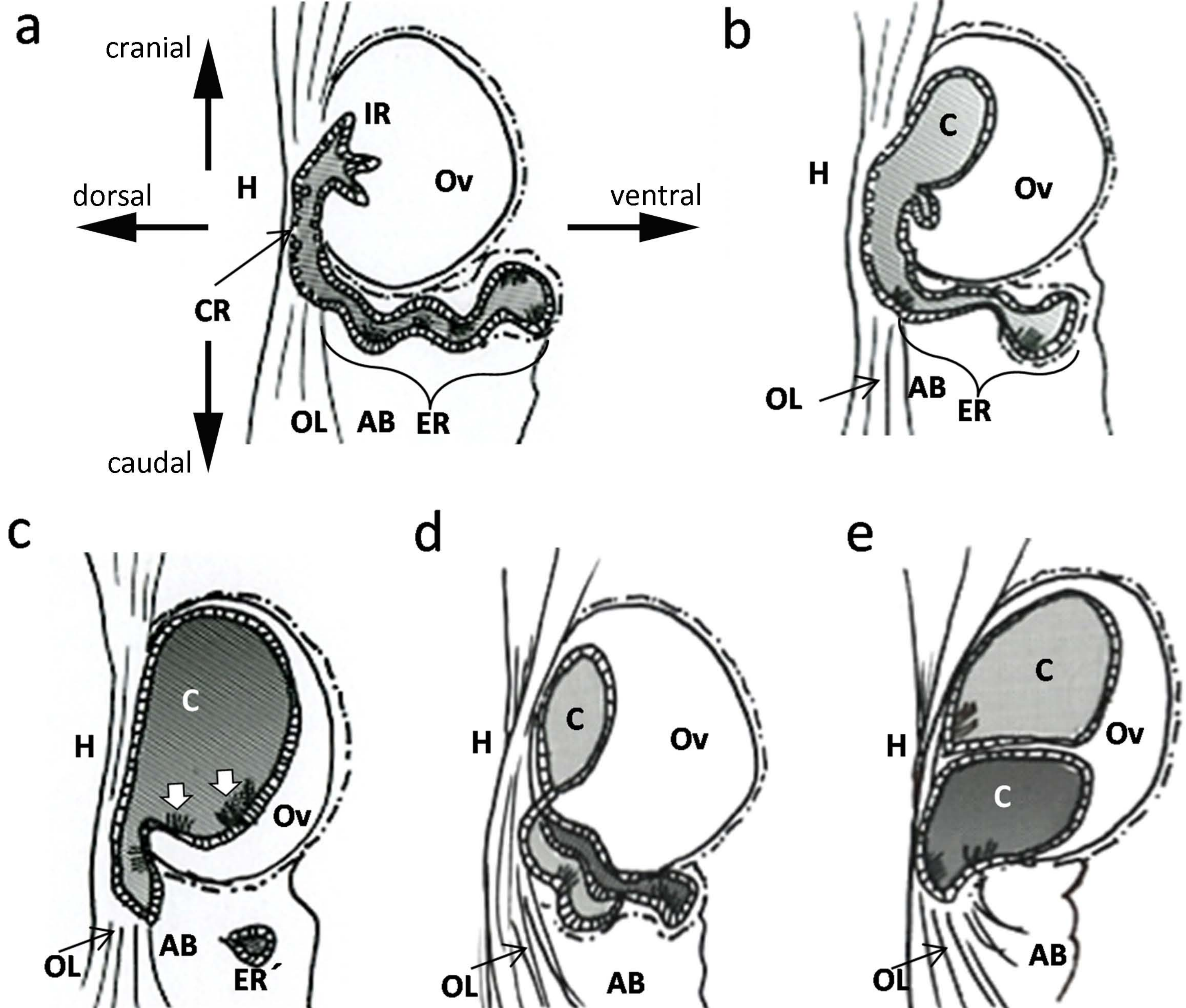


Table 1. The relationship between ER morphology and circumference of the IR in B6 and MRL mice at various ages.

Strain	Rete ovarii		Ages		
			2 weeks ~ 3 months	4 ~ 8 months	9 ~ 12 months
B6	ER morphology	regressive	ND	9%	ND
		simple	15%	ND	30%
		developed	85%	91%	70%
	IR or intraovarian	Circumference (mm)	1.0 ± 0.2	0.9 ± 0.1	0.8 ± 0.1
MRL	ER morphology	regressive	6%	18%	66%
		simple	79%	77%	17%
		developed	15%	5%	17%
	IR or intraovarian	Circumference (mm)	1.3 ± 0.1	4.3 ± 0.6	22.2 ^{a,b*} ± 5.3

Total of 35 ovaries in B6 and 61 ovaries in MRL mice were used. ND = not detected. a: significantly different with “2 weeks ~ 3 months”, b: significantly different with “4 ~ 8 months”. *: $P < 0.0001$ by the Kruskal-Wallis test, Schéffe’s method, values = means ± S.E.